J. Min. Metall. Sect. B-Metall. 53 (1) B (2017) 47 - 52

Journal of Mining and Metallurgy,
Section B: Metallurgy

CHARACTERIZATION OF THE EXPANDED AUSTENITE DEVELOPED ON AISI 316 LM STEEL BY PLASMA NITRIDING

M. Keddam[a*], T. Thiriet[b], G. Marcos[b], T. Czerwiec[b]

[a] Laboratoire de Technologie des Matériaux, Faculté de Génie Mécanique
et Génie des Procédés, Algeria
[b] Institut Jean Lamour (IJL), Université de Lorraine, Nancy Cedex, France

(Received 15 November 2015; accepted 18 October 2016)

Abstract

AISI 316 LM samples were plasma nitrided at a temperature of 380°C for different times between 0.5 and 8 h in a 85%N_2-15% H_2 gas mixture. Different experimental techniques such as: optical microscopy (OM), X- ray diffraction (XRD) and glow discharge optical emission spectroscopy (GDOES) were used to characterize the expanded austenite layer formed at the surface of AISI 316 LM stainless steel. The microscopical observations revealed the presence of the expanded austenite with a mean layer thickness between 1.90 and 4.31 μm. The growth kinetics of expanded austenite was also investigated. In addition, both the compressive stresses in the expanded austenite layer and the compositional strains were estimated by means of a simple mechanical model based on the XRD results.

Keywords*: Plasma nitriding; Expanded austenite; Kinetics; Mechanical model; Stress; Strain*

1. Introduction

Plasma Nitriding is one of the widely used surface treatments methods to improve the surface hardness and wear resistance of various engineering materials such as austenitic stainless steels. These materials are widely employed in many industrial areas such as offshore installations, construction industry and chemical tankers due to their very high general corrosion resistance [1–3]. Unfortunately, their low hardness and poor wear resistance seriously limit these applications [4–8].

Austenitic stainless steels can also be employed in orthopedics since they have good mechanical properties and they are biocompatible [9]. The plasma nitriding techniques are known to improve both surface hardness and corrosion resistance of austenitic stainless steels at low temperatures. As a consequence, a modified surface layer essentially composed of a metastable phase, known as supersaturated or expanded austenite [10-17] or S-phase [18-21] is formed without loosing the resistance to corrosion.

The expanded austenite, which is the nitrogen-rich phase, is the result of nitrogen atoms occupying the fcc octahedral sites until the saturation level is reached [22]. This diffusion of nitrogen atoms leads to the distortion of crystalline structure by inducing a high density of stacking faults.

It is known that the properties of expanded austenite depend on the used gas mixture. For indication, Negm [23] investigated the effect of (H_2/N_2) pressure ratios on the plasma nitriding of AISI 304 steel. He said that the addition of hydrogen up to 50%, might improve the efficiency of plasma nitriding. Hudis [24] also concluded that the addition of hydrogen gas to nitrogen gas provides more effective cleaning of treated samples. Furthermore, it is reported that the growth kinetics of compound layers on AISI 316 steel is increased with increasing N_2 content in the gas mixture up to approximatively 80% [25].

The present work focuses on the experimental study of the expanded austenite formed on AISI 316LM steel after plasma nitriding at 380°C in a 85%N_2-15% H_2 gas mixture for different treatment times (from 0.5 to 8 h). The growth kinetics of expanded austenite was also studied. In addition, a mechanical model was used to estimate the compressive stresses and compositional strains induced by nitrogen diffusion.

* *Corresponding author: mkeddam@usthb.dz*

DOI:10.2298/JMMB151115026K

2. Experimental details

The material used in the present investigation is AISI 316 LM austenitic stainless steel having a chemical composition given in Table 1. AISI 316 LM means a medical grade stainless steel. The material was received in the form of a cylindrical rod and was machined into test samples of 20 mm diameter and 5 mm thick.

Table 1. Chemical composition of AISI 316 LM austenitic stainless steel (given in weight percent)

Fe	C	Mn	Si	S	P	Cr	Ni	Mo	Cu	N
62.72	0.017	1.79	0.38	<0.002	0.019	17.43	14.7	2.74	0.16	0,04

Before plasma nitriding, the samples wet grounded using a series of emery papers down to 1200 grade, followed by fine polishing using 3 µm diamond paste. Afterwards, they were ultrasonically cleaned with alcohol and rinsed with distilled water in succession before being placed into the reactor chamber.

Plasma nitriding was carried out using a 800 Hz pulsed d.c. discharge, with a 0.8 duty cycle ratio (ratio of the pulse duration to the pulse period). The nitriding treatments were performed under a working pressure of 3 mbar in a mixture of (85%N_2-15% H_2). The voltage applied between cathode and anode was between 490 and 500 V with a current intensity of 0.20 A. The sample temperature was controlled during the treatment using a thermocouple embedded in the substrate holder. At the end of the treatment, the samples were slow cooled down under vacuum.

The microstructure and morphology of the nitrided samples were examined under an optical microscope (OLYMPUS VANOX AHMT3). Before microscopic examination, the polished cross-sections of the samples were etched for 2 min in the Curran reagent ($FeCl_3$ 30 g + HCl 30 ml + H_2O 120 ml). The thicknesses of the nitrided layer were measured by cross-sectional micrographs at several different zones.

In order to identify the phases present in the nitrided layer, the XRD analysis was carried out using a Philips X-ray diffractometer with a Co-Kα radiation (λ_{Co} =0.178889 nm) in a conventional θ–2θ Bragg-Brentano symmetric geometry.

Composition depth-profile analysis was carried out by means of Glow Discharge Optical Emission Spectrometry (GDOES) using JOBIN YVON 1000 RF PROFILER analyzer. This equipment was calibrated for all the alloying elements found in stainless steel with special attention to nitrogen element.

3. Experimental results and discussion

3.1 Microscopic observations of the expanded austenite

Figure 1 shows the optical micrographs of the cross-sections of the plasma nitrided samples at 380° C for increasing times (from 0.5 to 8 h). It reveals the formation of nitrogen–rich phase called expanded austenite after etching with the Curran reagent.

The nitrided layer looks very dense and continuous with a difference in thickness depending on the treatment time. This thickness reached a value of 4.31 µm after 8 h of treatment while it was only of 1.90 µm for 0.5 h of treatment. In comparison, Wang et al.[26] have obtained a layer thickness close to 2.3 µm for the expanded austenite layer when plasma nitriding the AISI 304L steel at 420 °C for 0.5 h. Keddam et al. [17] have obtained a thickness of 9.7 µm during 8 h at 420 °C for the expanded austenite formed in AISI 316 L steel when using a 90%N_2-10% H_2 gas mixture. In addition, Nosei et al. [27] have plasma nitrided the AISI 316 L steel using a gas mixture of (25%N_2+75%H_2) and obtained an expanded austenite layer of approximatively 5 µm in thickness for 0.5 h of treatment at 400 °C. It puts in evidence that the gas composition exerts an influence on the growth kinetics of expanded austenite.

3.2 The growth kinetics of expanded austenite

Figure 2 describes the time dependence for the thickness of expanded austenite. The growth law of

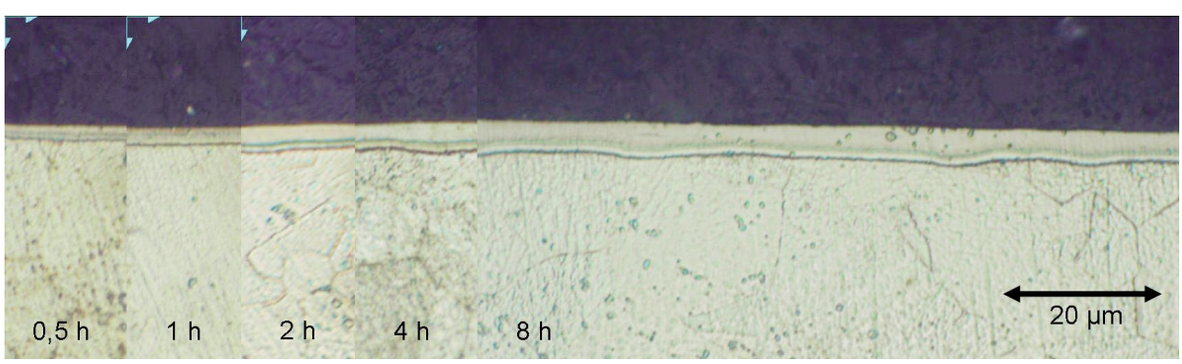

Figure 1. *Optical micrographs of the cross-sections of the nitrided samples at 380°C for different times: (a) 0.5 h, (b) 1 h, (c) 2 h, (d) 4 h and (e) 8 h*

this layer can be given by Equation (1):

$$u = 1.6774\sqrt{t} \quad (1)$$

where the variable u denotes the layer thickness of expanded austenite in (μm) and t the treatment time in hour. Assuming a semi infinite medium [28], in which the nitrogen diffusion proceeds through the layer of expanded austenite, the effective diffusion coefficient of nitrogen in the expanded austenite can de obtained by identifying Equation (1) to Equation (2).

$$u = 2\sqrt{D_N^{\gamma_N} t} \quad (2)$$

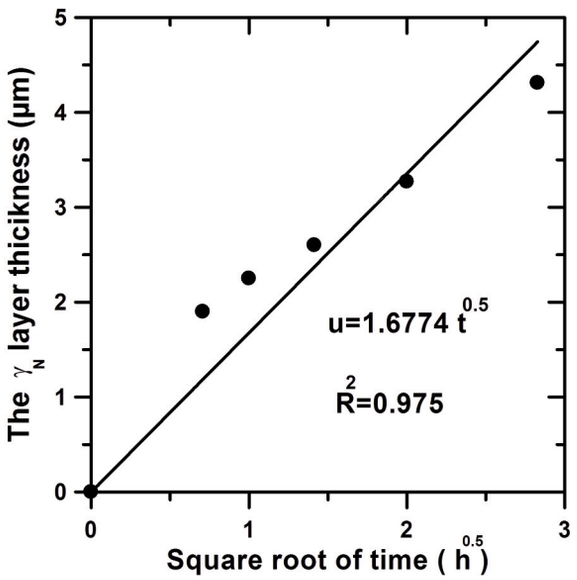

Figure 2. *The time dependence for the layer thickness of expanded austenite*

The value of 1.95×10^{-12} cm^2s^{-1} was determined as the effective nitrogen diffusion coefficient in the expanded austenite at 380°C. By this way, Keddam et al. [17] have obtained a value of 11.1×10^{-12} cm^2s^{-1} at 420°C when using a gas mixture of ($90\%N_2 + 10\%H_2$) for AISI 316 L steel. In addition, Moskalioviene et al. [29] have evaluated the nitrogen diffusion coefficient in AISI 316 L stainless steel at 400°C treated by plasma nitriding process using a gas mixture of ($60\%N_2 + 40\%H_2$). Using the kinetic data reported by these authors [29], the diffusion coefficient of nitrogen in the expanded austenite was estimated as 4.8×10^{-12} cm^2s^{-1} at 400°C from Equation (2).

3.3 XRD analysis

Figure 3 gives the XRD patterns of the samples plasma nitrided at 380°C for different times (from 0.5 to 8 h). In the plasma nitrided samples, the γ(111) and γ(200) peaks were shifted towards lower angles, suggesting the expansion of the fcc lattices by dissolved nitrogen atoms. So, the presence of expanded austenite was evidenced by the diffracting peaks with a shift of 2Θ angles towards lower values compared to the diffracting peaks of austenite phase. This behaviour can be explained by a high distortion of the austenite lattice due to the incorporation of a large amount of nitrogen concentration [30-32]. In addition, the shift of the austenite peaks to lower angles indicates compressive residual stresses in the nitrided layer. The broad diffraction peaks corresponding to the expanded austenite can be observed in addition to austenite reflections from the substrate material. This broadening is probably due to the gradient of nitrogen concentration through the nitrided layer.

Based on XRD results, there is only a single phase (expanded austenite) at the surfaces of AISI 316 LM steel nitrided at 380°C with a gas mixture of ($85\%N_2 + 15\% H_2$).

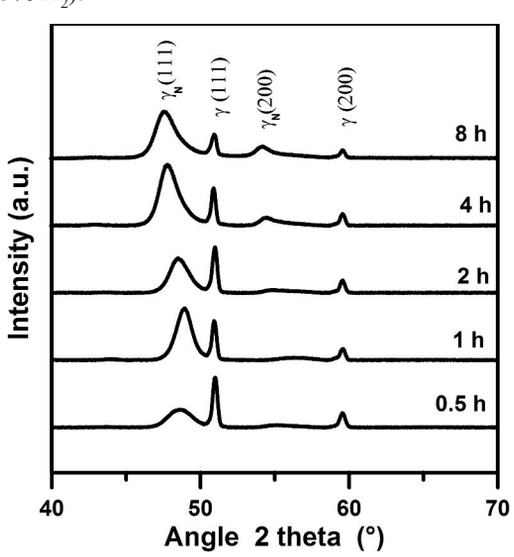

Figure 3. *XRD patterns of the samples nitrided at 380°C for different treatment times*

3.4 GDOES profiles

Figure 4 displays the nitrogen profiles obtained by GDOES analysis on the surfaces of the samples nitrided at 380°C for increasing treatment times.

It is seen that the layer thickness of expanded austenite linearly varies with the square root of treatment time. This result is compatible with the microscopic observations (see Figure 1) where the layer thickness of expanded austenite is increased as the time duration changes from 0.5 to 8 h. Furthermore, the nitrogen concentration at the material surface rises with the treatment time due to the dissolution of a large amount of nitrogen atoms in the lattice of expanded austenite (see Figure 4).

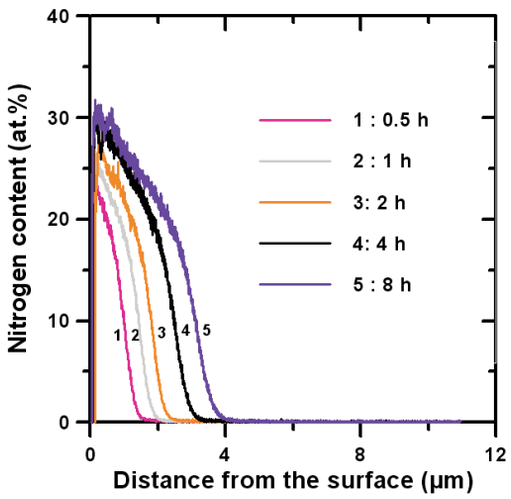

Figure 4. *The nitrogen profiles obtained by GDOES analysis on the surfaces of the samples nitrided at 380°C for increasing treatment times*

4 The mechanical model

To evaluate the compressive stress and the compositional strain induced by the nitrogen diffusion in the layer of expanded austenite, a mechanical model recently developed by Czerwiec et al. [33] was used for this purpose. This model, based on the Hooke's law, considers a planar stress state in the layer of expanded austenite. In the X-ray diffraction reference frame and a θ-2θ configuration with non zero ψ angle, the mean elastic diffraction strain is given by Equation (3) in case of the quasi-isotropic samples [34]:

$$< \varepsilon_{\Psi}^{hkl} >= 2S_1^{hkl} < \sigma > + \frac{1}{2} S_2^{hkl} < \sigma > \sin^2(\Psi) \quad (3)$$

$$S_1^{hkl} = (S_{12} + S_0 A_{hkl}) \quad (4)$$

The A_{hkl} parameter given by Equation (5) depends on the Miller indexes of the [h k l] crystallographic direction as follows:

$$A_{hkl} = \frac{(hk)^2 + (hl)^2 + (kl)^2}{(h^2 + k^2 + l^2)^2} \quad (5)$$

$$S_2^{hkl} = (S_{11} - S_{12} - 3S_0 A_{hkl}) \quad (6)$$

$$S_0 = (S_{11} - S_{12} - 0.5S_{44}) \quad (7)$$

The numerical values of mechanical constants [35, 36] involved in equations (6) and (7) are listed in Table 2.

Table 2. Constants used in the mechanical model taken from references [35] and [36]

Constants	S_0	S_{11}	S_{12}	S_{44}
Unit (Pa^{-1})	1.065×10^{-11}	10.7×10^{-12}	-4.25×10^{-12}	8.6×10^{-12}

The mean elastic diffraction strain is the difference between the mean total strain in the [h k l] direction and the dilatational or compositional strain given by Equation (8):

$$< \varepsilon_{\Psi}^{hkl} >=< \varepsilon_{[hkl]}^{t} > - < \varepsilon^{C} > \quad (8)$$

The mean lattice parameter, determined by X–Ray diffraction, is related to the mean total strain in the [h k l] direction by Equation (9):

$$< a^{hkl} >= a_0[1 + < \varepsilon_{[hkl]}^{t} >] \quad (9)$$

By the same way, the isotropic stress free lattice parameter of the expanded austenite related to the compositional strain, can be obtained from Equation (10) as follows:

$$< a(C_N, \sigma = 0) >= a_0[1 + < \varepsilon^{C} >] \quad (10)$$

where a_0 is the lattice parameter of the substrate (a_0= 0.359 nm for AISI 316 LM steel).

For an angle of ψ= 0 in a θ-2θ configuration for the X-ray diffraction reference. The expression of the mean lattice parameter can be expressed by Equation (11):

$$< a^{hkl} >= a_0[1 + 2S_{12} < \sigma > + < \varepsilon^{C} >] + 2S_0 < \sigma > a_0 A_{hkl} \quad (11)$$

A linear relation was observed experimentally between the mean lattice parameter and the orientation factor given by Equation (12):

$$< a^{hkl} >= \alpha + \beta A_{hkl} \quad (12)$$

By identifying Equation (11) to Equation (12), it is possible to deduce the values of the compressive stress and the compositional strain as follows:

$$< \sigma >= \frac{\beta}{2S_0 a_0} \quad (13)$$

and

$$< \varepsilon >= [\frac{\alpha}{a_0} - \frac{S_{12}\beta}{S_0 a_0} - 1] \quad (14)$$

In addition, a linear relation exists also between the mean nitrogen concentration C_N (at.%) in the expanded austenite and its lattice parameter (in nm) according to Picard's relation [37] :

$$a_{\gamma_N} = (0.3587 + 9\times10^{-4} C_N) \quad (15)$$

By identifying $< a(C_N, \sigma=0) >$ from Equation (10)) to the lattice parameter of expanded austenite from Equation (15), the mean nitrogen concentration in the expanded austenite can be readily determined.

4.1 Determination of the compressive stresses and the compositional strains in the expanded austenite

The expanded austenite once formed on the surface substrate exerts a compressive state on the non nitrided core. The nitrogen diffusion significantly affects the stress state of the modified surface via the plasma nitriding treatment. The resultant misfit must be elastically accommodated to maintain the layer of expanded austenite attached to the rest of substrate. The mechanical model presented here constitutes a simple tool for studying the mechanical properties of the expanded austenite. The present model was then used to estimate the compressive stresses in the expanded austenite and the compositional strains. Table 3 lists the calculated values of compressive stresses along with the induced compositional strains obtained by the mechanical model for the samples nitrided at 380°C for different times (from 0.5 to 8 h).

Table 3. Estimation of the compressive stresses, the compositional strains in the expanded austenite and its nitrogen concentration as a function of the treatment time at 380°C

Time (h)	$\prec\sigma\succ$ (GPa)	$\prec\varepsilon\succ$	$a_{\gamma_N}(200)$ (nm)	$a_{\gamma_N}(111)$ (nm)	$C_N(at.\%)$ Equation (15)
0.5	-3.79	0.0395	0.3848	0.3751	16.1
1	-2.13	0.0365	0.3786	0.3732	14.8
2	-4.18	0.0424	0.387	0.3763	17.2
4	-3.12	0.0593	0.3898	0.3818	24
8	-3.51	0.0606	0.3915	0.3826	24.5

The calculated values of compressive stresses in the expanded austenite are ranging from 2.13 to 4.18 GPa while the values of compositional strains are between 3.65 and 6.06 %. In Table 3, the calculated values of mean nitrogen concentration in the expanded austenite were determined using Equation (15).

From Table 3, it is noted that the calculated values of compressive stresses are depending on the treatment time. However, a lower value of the compressive stress (=2.13 GPa) was obtained for a treatment time of 1 h. This fact can be ascribed to the stress relaxation induced by plastic deformation of the expanded austenite layer. In this sense, Borgioli et al. [15] showed that the presence of slip lines observed by optical micrographs in a plasma nitrided of austenitic stainless steel is the consequence of the development of compressive stresses in the expanded austenite.

When the residual stress, induced by the formation of expanded austenite, exceeds the maximum yield stress, a plastic deformation occurs giving rise to slip lines and stacking faults. In fact, these stacking faults can be considered as partly responsible for the X-ray diffraction peaks shifting from the free stress lattices. This effect can be observed by the set of slip bands developed within the grains of treated sample [38].

Keddam et al. [17] have plasma nitrided the AISI 316 L steel using a gas mixture of (90%N_2+ 10% H_2) and they have estimated the values of compressive stresses for the expanded austenite. The authors have noticed that the values of compressive stresses in the expanded austenite are influenced by the gas composition. The estimated values of compressive stresses obtained by Keddam et al. [17] are slightly different from the results displayed in Table 3 for the plasma nitrided AISI 316 LM steel. For indication, the maximum value of estimated compressive stress was 3.7 GPa for 2 h of treatment with a gas mixture of (90%N_2+ 10% H_2 gas) for AISI 316 L steel [17].

In the present work, the maximum value of estimated compressive stress is 4.18 GPa for 2 h at 380°C with a gas mixture of (85%N_2+ 15% H_2) for AISI 316 LM steel.

It is clearly seen that the proportion of H_2 in the gas mixture exerts an influence on the dissolution rate of nitrogen at the surface of treated material. The values of mean nitrogen concentrations calculated from Equation (15) are influenced by the time duration.

Table 4 shows a comparison between the mean values of nitrogen concentrations in the expanded austenite taken from the GDOES curves and those estimated from the XRD results

A discrepancy was then observed between the results from the GDOES analysis and those obtained by the XRD analysis. In fact, the XRD results did not take into account the averaged values resulting from the penetration of Co-Kα radiation in the material.

Table 4. Estimation of the mean values of nitrogen concentrations for the expanded austenite by two methods at different times

Time (h)	$C_N(at.\%)$ from GDOES analysis	$C_N(at.\%)$ from XRD analysis
0.5	23	16.1
1	26	14.8
2	27	17.2
4	30	24
8	30	24.5

4. Conclusions

In the present investigation, the AISI 316 LM steel was plasma nitrided at 380°C between 0.5 and 8 h in a 85%N_2-15% H_2 gas mixture. Based on the XRD

studies, the expanded austenite was formed on the surfaces of AISI 316 LM steel having a mean thickness between 1.90 and 4.31 μm. It is found that expanded austenite layer obeyed the parabolic growth law.

The GDOES analyses showed an increase in the layer thickness with the treatment time.

A mechanical model was used to determine both the compressive stresses, induced by the nitrogen diffusion, and the compositional strains in the expanded austenite. As a result, the estimated compressive stresses inside the expanded austenite layer (in absolute values) are between 2.13 and 4.18 GPa, while the values of compositional strains are ranging from 3.65 to 6.06 %.

References

[1] M. Cindra Fonseca, I.N. Bastos, E. Baggio-Saitovitch, D.R. Sánchez , Corrosion Science 55 (2012), 34-39.

[2] N.R. Baddoo, Journal of Constructional Steel Research 64 (2008), 1199-1206.

[3] P. Boillot and J. Peultier, Procedia Engineering, 83 (2014), 309-321.

[4] T. Bell, Surface Engineering 18 (2002), 415–422.

[5] S. Corujeira Gallo, X. Li, H. Dong, Tribology Letters 45 (2012), 153–160.

[6] S. Corujeira Gallo, H. Dong, Applied Surface Science 258 (2011), 608–613.

[7] A. Devaraju, A. Elaya Perumal, J. Alphonsa, S.V. Kailas, S. Venugopal, Wear 288 (2012), 17–26.

[8] D. Zeng, S. Yang, Z.D. Xiang, Applied Surface Science 258 (2012), 5175–5178.

[9] S. Kožuh, l. Vrsalović, M. Gojić, S. Gudić , B. Kosec, J. Min. Metall. Sect. B-Metall. 52 (1) B (2016), 53 – 61.

[10] A.M. Kliauga, M. Pohl, Surf. Coat. Technol. 98 (1998), 1205-1210.

[11] T. Bell, Y. Sun, Heat Treat. Met. 29 (2002), 57-64.

[12] M.P. Fewell, D.R.G. Mitchell, J.M. Priest, K.T. Short, G.A. Collins, Surf. Coat. Technol. 131 (2000), 300-306.

[13] S. Kumar, M.J. Bladwin, M.P. Fewell, S.C. Haydon, K.T. Short, G.A. Collins, J. Tendys, Surf. Coat. Technol. 123 (2000), 29-35.

[14] D. Manova, S. Mandl, H. Neumann, B. Rauschenbach, Surf. Coat. Technol. 200 (2006), 6563-6567.

[15] F. Borgioli, A. Fossati, E. Galvanetto, T. Bacci, Surf. Coat. Technol. 200 (2005), 2474-2480.

[16] G.P. Singh, J. Alphonsa, P.K. Barhai, P.A. Rayjada, P.M. Raole, S. Mukherjee, Surf. Coat. Technol. 200 (2006), 5807-5811.

[17] M. Keddam, G. Marcos, T. Thiriet, T. Czerwiec, H. Michel, Matériaux et Techniques 101, 204 (2013).

[18] E. Menthe, U.A. Bulak, J. Olfe, A. Zimmermann, K.T. Rie, Surf. Coat. Technol. 133–134 (2000), 259-263.

[19] T. Bacci, F. Borgioli, E. Galvanetto, G. Pradelli, Glow-discharge nitriding of sintered stainless steels, Surf. Coat. Technol. 139 (2001), 251-356.

[20] C.X. Li, T. Bell, Corros. Sci. 46 (2004), 1527-1547.

[21] A. Martinavicius, G. Abrasonis, A.C. Scheinost, R. Danoix, F. Danoix, J.C. Stinville,G. Talut, C. Templier, O. Liedke, S. Gemming, W. Möller, Acta Materialia 60 (2012), 4065–4076.

[22] J. García Molleja, M. Milanese, M. Piccoli, R. Moroso, J. Niedbalski, L. Nosei, J. Bürgi, E. Bemporad, J. Feugeas, Surf. Coat. Technol. 218 (2013), 142–151

[23] N.Z.Negm, Materials Science and Engineering B 129 (2006), 207–210

[24] M. Hudis, J. Appl. Phys. 44 (1973), 1489-1496.

[25] R.R.M. de Sousa, F.O. de Araújo, L.C. Gontijo, J.A.P. da Costa, C. Alves Jr, Vacuum 86 (2012), 2048-2053

[26] L. Wang, S. Ji, J. Sun, Surf. Coat. Technol., 200 (2006), 5067-5070.

[27] L.Nosei, M. Avalos, B.J. Gomez, L. Nachez, J. Feugeas, Thin Solid Films 468 (2004) 134– 141

[28] P. Shewmon, Diffusion in Solids, Minerals, Metals and Materials Society,USA,1999.

[29] T. Moskalioviene, A. Galdikas, J.P. Rivière, L. Pichon, Surf. Coat. Technol. 205 (2011), 3301-3306.

[30] H. Dong, International Materials Reviews 55 (2010), 65–98.

[31] Y. Sun, X.Y. Li, T. Bell, Journal of Materials Science 34 (1999), 4793–4802.

[32] Yang Li, Zhuo Wang, Liang Wang, Applied Surface Science 298 (2014), 243–250

[33] T. Czerwiec, H. He, G. Marcos, T. Thiriet, S. Weber, H. Michel, Plasma Process. Polym. 6 (2009), 401-409.

[34] V. Hauk, Structural and Residual Stress Analysis by Non destructive Methods, Elsevier, Amsterdam, 1997.

[35] V. Rejevac, M. Hoelzel, S.A. Danilkin, A. Hoser, H. Fuess, J. Phys. Condens. Matter, 16 (2004) 2609-2616.

[36] A. Teklu, H. Ledbetter, S. Kim, L.A. Boatner, M. McGuire, V. Keppens, Mett. Mat.Trans. A 35 (2004), 3149-3154.

[37] S. Picard, J.B. Memet, R. Sabot, J.L. Grosseau-Poussard, J.P. Rivière, R. Meilland, Materials Science And Engineering A 303 (2001), 163-172.

[38] J. Feugeas, L. Rico, L. Nosei, B. Gómez, E. Bemporad, J. Lesage, J. Ferrón, Surface and Coatings Technology 204 (2010), 1193–1199